Quark Loop Dynamics and Meson Decays *

H. Suura +

Deutsches Elektronen-Synchrotron DESY, Hamburg

and

Bing-Lin Young ++

Department of Physics, Iowa State University, Ames, Iowa 50010

* Work assisted in part by the U.S. Atomic Energy Commission

+ On leave from School of Physics and Astronomy, University of Minnesota, Minneapolis, Minnesota 55455

++ Work performed at Ames Laboratory of the U.S. Atomic Energy Commission

DISCLAIMER

Abstract

From a set of lowest order quark loop diagrams for static mesonic amplitudes involving vector and axial-vector vertices, we determine the effective quark mass and the meson-quark-quark coupling constants for three types of quark models. These parameters are applied to evaluate certain mesonic decays and the SU_3 mass splitting of 0^- octet and 1^- nonet, which serve as tests for the quark models. Adler's low energy theorem for the $\pi^0 \to 2\gamma$ decay is derived in our approach without invoking the Adler-Schwinger anomaly. The test favors the Nambu-Han model of integrally charged quarks. Critical examinations of the underlying assumption of the quark loop dominance are made, and a speculation on a physical model which allows such a situation will be proposed.

I. Introduction

The Sutherland puzzle[1] concerning $\pi^o \to 2\gamma$ decay was resolved by Adler[2] through the modified PCAC condition taking into account the Adler-Schwinger anomaly[3] of the divergence of the axial-vector currents. It gives the $\pi^o \to 2\gamma$ amplitude, T_π [4], in terms of the pion decay constant f_π as

$$T_\pi = \frac{\alpha}{\pi} \frac{m_\pi}{f_\pi} S, \qquad (1)$$

where S is a number critically dependent on the charge of quarks involved. Okubo[5] used Eq.(1) and a related amplitude for $\omega \to \pi^o + \gamma$ as critical tests for a variety of quark models. (This paper will be referred to in the following as O). In using Eq.(1) to test quark models, however, the central question is how to justify it in the context of quark models. Okubo merely noted that the pseudoscalar-meson-quark-quark, πqq, coupling constant consistent with the modified PCAC condition was $\sqrt{2}/f_\pi$ and that the $\pi^o \to 2\gamma$ triangular diagram with this coupling constant gave Eq.(1). The crucial point is then a determination of the coupling constant. We may remark in this connection that the old Fukuda-Miyamoto and Steinberger calculation[6] of $\pi^o \to 2\gamma$ by a nucleon loop diagram can be converted into Eq.(1) if one eliminates πNN coupling constant in terms of f_π by the Goldberger-Treiman relation[7] and neglects all renormalization effects. Again to apply this scheme to quarks we will have to find the πqq coupling in the context of a quark model.

In our present paper, we would like to take a general approach which may be called a quark-loop dynamics to deal with static mesonic amplitudes. We assume that such amplitudes like $\pi^+ \to \mu^+\nu$, $\rho_o \to \gamma$, $\pi^+ \to \pi^+\gamma$, $\rho^+ \to \rho^+\gamma$, $\rho^o \to \pi^+\pi^-$, $\pi^o \to 2\gamma$, $\omega \to \pi^o\gamma$, etc., are dominated by the corresponding lowest order quark-loop diagrams, with certain cut-offs if necessary. Our scheme is somewhat related to the so-called relativistic quark models[8], where conventionally a certain simplified relativistic structure is assumed for a meson wave function including two quark legs. In calculating loop diagrams with these wave functions the quark propagators are hidden in the scalar part of the wave function, and momentum integration is eventually parametrized. In our approach, on the other hand, we assume a direct $\gamma_5(\gamma_\mu)$ coupling for $\pi qq(\rho qq)$ vertex and fully take into account the quark propagators. We will discuss a possible physical

significance of the effects of such quark propagations in sections III and IV. The hypothesis of the dominance of the lowest order diagrams may be justified in the following sense. We have a vector gluon model [9] in mind. We may then expect that because of the Ward identity, the renormalization effects of the vector and the axial-vector vertices are small. Specifically, it will not be necessary to saturate vertices by vector or axial-vector mesons, at least as long as we deal with normalization at zero momentum-transfer squared, which we are going to do. Renormalization at a meson vertex can be incorporated into the meson-quark-quark coupling constant. Thus, we are neglecting essentially radiative corrections across two channels, which we expect to be small.

The cut-off must be given a real physical meaning in order for our scheme to make sense. We do not know a precise mechanism for the cut-off, expect for a vague statement that it reflects a certain structure of mesons. Fortunately, our result is remarkably independent of different cut-off methods as will be discussed in detail in the next section and in the appendix. We evaluate loop diagrams neglecting terms inversely proportional to the cut-off mass but retaining finite constant terms. In the limit of vanishing external meson masses, we obtain remarkably simple relations for the coupling constants which reproduce Eq(1) and the $\omega \to \pi^0\gamma$ amplitude used in O. Thus the analysis of the various quark models made there remains to be valid. We will also study effects of the finite constant terms which are functions of the ratios of external meson masses to the quark mass. Keeping such terms, we can determine the quark mass for each quark model we study, which turns out to be slightly larger than half of the ρ mass in each case. Because of the closeness of ρ mass to the pseudo-threshold for $\rho \to q + \bar{q}$, certain amplitudes are strongly enhanced. However, the overall effect is such that physical amplitudes are not greatly affected. The physical significance of this will be discussed in section IV. We will find in the following, a remarkably simple and consistent picture in this most simple-minded approach, provided a certain three-triplet model involving integrally charged quarks is used. In section V we will examine our fundamental assumption of the quark-loop dominance and propose a speculative physical situation in which such assumption might be justified.

II. Description of Method and Models

The diagrams mentioned in the previous section are all at most superficially linearly divergent, after imposing a gauge condition on the ρ^0-γ loop diagram

with the ρ mass temporarily off the mass shell. The latter condition is necessary, because without it the photon propagator would acquire a mass through ρ intermediate state. Then, with an appropriate cut-off Λ, the dimensionless part of a diagram i will have a form

$$\ell n \left(\frac{\Lambda^2}{M^2}\right) + A_i + B_i \left(\frac{m^2}{M^2}\right) + O\left(\frac{1}{\Lambda^2}\right) , \tag{2}$$

where M is a quark mass involved and m is an external meson mass. B_i, a function of m^2/M^2, becomes <u>independent</u> of the cut-off method, if further specified by requiring

$$B_i\ (m^2/M^2) = 0 \quad \text{for} \quad m^2/M^2 \to 0. \tag{3}$$

A_i is then a numerical constant by definition; its value depends on the cut-off method. Although the value of A_i changes widely for different cut-off methods, it changes remarkably little for different diagrams once a particular cut-off method is chosen. Thus we can combine the bulk of A say $\bar{A}$, with $\ell n(\Lambda^2/M^2)$ and write (2) in the form

$$L + \Delta A_i + B_i \left(\frac{m^2}{M^2}\right) \tag{4}$$

with

$$L \equiv \ell n \left(\frac{\Lambda^2}{M^2}\right) + \bar{A} \tag{5}$$

and

$$\Delta A_i = A_i - \bar{A} . \tag{6}$$

Our whole scheme is based on the facts that ΔA_i is small and can be neglected, and also that there are only two cut-off parameters Λ_π and Λ_ρ, or $L\pi$ and $L\rho$ which can be easily eliminated. In the appendix, we will discuss two cut-off methods, which give, respectively,

$$\overline{A} = -1, -2.$$

As long as we neglect ΔA_i, it is obvious that the results are cut-off independent.

In view of the results already obtained by the analysis in 0, we will not examine all varieties of quark models, but choose three cases of most physical interest. They are the Gell-Mann - Zweig model of fractionally charged quarks and two versions of the three triplet model originally due to Nambu and Han [10]. In the latter, the three triplets, convenriently called S, U and B form a new SU_3 space, charm space, and they are assigned a charm quantum number C (corresponding to hypercharge in the ordinary SU_3 space) equal to 1, 1, -2 respectively. The Gell-Mann - Nishijima formula is modified to

$$Q = T_3 + \frac{1}{2} Y + \frac{1}{3} C \tag{7}$$

which gives quark charges $\begin{bmatrix} 1 \\ 0 \\ 0 \end{bmatrix}$, $\begin{bmatrix} 1 \\ 0 \\ 0 \end{bmatrix}$, and $\begin{bmatrix} 0 \\ -1 \\ -1 \end{bmatrix}$, respectively for S, U and B. The electromagnetic current is then

$$j_\mu^{em} = e \{ \bar{s}\gamma_\mu \begin{bmatrix} 1 \\ 0 \\ 0 \end{bmatrix} s + \bar{u}\gamma_\mu \begin{bmatrix} 1 \\ 0 \\ 0 \end{bmatrix} u + \bar{B}\gamma_\mu \begin{bmatrix} 0 \\ -1 \\ -1 \end{bmatrix} B \} \tag{8}$$

where S, U and B each represents a triplet of quark spinors.

Since the total charm quantum number C for any ordinary hadron must be zero, a charm space configuration of mesons must be restricted to either charm singlet or the eighth memeber of a charm octet. Since low lying states are not degenerate, we are anticipating here a rather large charm symmetry breaking or a singlet-octet mixing in order to allow for a case of the octet. However, for 1^- mesons (V) we must take a charm singlet, because otherwise we will have a non-vanishing contribution to V-γ coupling constants from the charm octet (and unitary singlet) component of the electromagnetic current. This would lead to a large deviation from SU_3 predicted ratio of ρ^0-γ, ω-γ and Φ-γ coupling constants, contrary to available experimental data. Thus, as Vqq interaction we take

$$Hvqq = g_v \left[\bar{S}\gamma_\mu \lambda_a S + \bar{U}\gamma_\mu \lambda_a U + \bar{B}\gamma_\mu \lambda_a B\right] \phi_a^\mu \tag{9}$$

where λ_a, a = 1,... 8, are SU_3 spin matrices (and $\lambda_o = \sqrt{\frac{2}{3}}\, I$), and ϕ_a^μ, a = 0, 1, ... 8 are nonet vector meson wave functions.

For 0^- mesons (P), the situation is not so simple. There is no a priori reason why they should be charm singlets [11]. We notice that the requirement of a chiral $SU_3 \times SU_3$ algebra for the weak vector and axial-vector currents dose not specify the relative signs of the S, U and B components of the axial-vector current. The following two versions of the Pqq interaction are related to this ambiguity.

Case I. A charm-singlet weak axial-vector current and a charm-singlet 0^- meson.

$$j_{5\mu}^{W,a} = \bar{S}\gamma_\mu\gamma_5\lambda_a S + \bar{U}\gamma_\mu\gamma_5\lambda_a U + \bar{B}\gamma_\mu\gamma_5\lambda_a B \tag{10}$$

and

$$Hpqq = ig_p \left[\bar{S}\gamma_5\lambda_a S + \bar{U}\gamma_5\lambda_a U + \bar{B}\gamma_5\lambda_a B\right] \phi_a, \tag{11}$$

where ϕ_a, a = 0,1,...8 are the singlet and octet pseudoscalar meson wave functions. This simplest case is most favored by any of the tests we make in section IV. The only drawback is that the radiative correction to the weak interaction is unrenormalizable in this model. As pointed out by several authors [12], in order for the electromagnetic radiative correction to be finite, one has to take V-A weak current for negatively charged quarks (B triplet in our case) and V+A for positively charged S and U triplets. The choice (11) gives only V-A or V+A.

Case II. We take a renormalizable axial current:

$$j_{5\mu}^{W,a} = -\bar{S}\gamma_\mu\gamma_5\lambda_a S - \bar{U}\gamma_\mu\gamma_5\lambda_a U + \bar{B}\gamma_\mu\gamma_5\lambda_a B \tag{12}$$

which is combined with a vector current in the form of $j^a_\mu - j^a_{5\mu}$ [13]. One might tempted to choose as 0^- state the same S, U and B mixture as in (12) so that an obvious PCAC holds. However, this choice leads to a too big $\pi^o \to 2\gamma$ amplitude and a too small $\omega^o \to \pi\gamma$ amplitude. We will choose, instead, a pure $B\bar{B}$ state [14] for 0^-, analogous to the ϕ meson configuration in the nonet quark model. This $B\bar{B}$ configuration for 0^- was studied before by Otokozawa and Suura [14].

$$Hpqq = i\, g_p\, \bar{B}\gamma_5\gamma_a\, B\, \phi_a. \tag{13}$$

Case III. Gell-Mann - Zweig model. We have a single triplet q.

$$j^{em}_\mu = e\bar{q} \begin{bmatrix} 2/3 & & \\ & -1/3 & \\ & & -1/3 \end{bmatrix} q, \tag{14}$$

$$j^a_\mu = \bar{q}\gamma_\mu\lambda_a\, q, \tag{15}$$

$$j^a_{5\mu} = \bar{q}\gamma_\mu\gamma_5\lambda_a\, q, \tag{16}$$

$$Hvqq = g_v\, \bar{q}\gamma_\mu\lambda_a\, q\, \phi^\mu_a, \tag{17}$$

and

$$Hpqq = i\, g_p\, \bar{q}\gamma_5\lambda_a\, q\, \phi_a. \tag{18}$$

III. Determination of Parameters

Coupling constants are derived from combinations of two-point loops for $\pi^+ \to \mu^+\nu$ and $\rho^o \to \gamma$, and triangle loops for $\pi^+\gamma \to \pi^+\gamma$ and $\rho^+ \to \rho^+\gamma$. The latter diagrams are used here to utilize a normalization condition for a charge. Using the current-quark-quark and meson-quark-quark couplings defined for the three cases in section II, it is a straight-forward matter to calculate these amplitudes. We neglect ΔA_i term in Eq.(4) and it does not matter in this approxi-

mation which cut-off to use. We obtain respectively for the three cases

$$f_\pi = -\begin{bmatrix}3\\1\\1\end{bmatrix} \frac{1}{4\pi^2}\, g_\pi M_1 L_\pi, \tag{19}$$

$$F_\pi(o) = 1 = \begin{bmatrix}3\\1\\1\end{bmatrix} \frac{1}{4\pi^2}\, g_\pi^2\, L_\pi, \tag{20}$$

$$\frac{1}{f_\rho} = \begin{bmatrix}3\\3\\1\end{bmatrix} \frac{g_\rho}{12\pi^2}\, [L_\rho + \tfrac{1}{2} I_o(\xi) - I_1(\xi) - 4I_2(\xi)]\ , \tag{21}$$

$$1 = \begin{bmatrix}3\\3\\1\end{bmatrix} \frac{g_\rho^2}{6\pi^2}\, [L_\rho + \tfrac{1}{2} I_o(\xi) - I_1(\xi) + 2I_2(\xi)]\ , \tag{22}$$

where L_π and L_ρ are cut-off parameters as defined in (5). f_ρ is the ρ^o-γ coupling constant defined in the usual way. M_1 is the p-(or n-)quark mass, and ξ is

$$\xi \equiv \frac{m_\rho^2}{M_1^2} \tag{23}$$

which we consider to be a variable parameter with m_ρ rather than M_1 changing. $I_n(\xi)$ is defined by

$$I_n(\xi) \equiv \xi \int dx\ \frac{[x(1-x)]^n}{1-\xi x(1-x)} \tag{24}$$

We have omitted the ξ dependent B type terms (cf.Eq.(3)) in (19) and (20), because there $\xi = m_\pi^2/M_1^2$ is very small. Combining (19) and (20) we obtain

$$\frac{g_\pi}{M_1} = -\begin{bmatrix}1\\1\\1\end{bmatrix} \frac{1}{f_\pi} \tag{25}$$

and

$$L_\pi = \ell n \left(\frac{\Lambda_\pi^2}{M_1^2} \right) + \bar{A} = \frac{4\pi^2 f_\pi^2}{M_1^2} \begin{bmatrix} 1/3 \\ 1 \\ 1 \end{bmatrix} \tag{26}$$

Eq. (25) is an equivalent of the Goldberger-Treiman relation [6], which gives Eq.(1) when used in $\pi^0 \to 2\gamma$ triangle diagram. In order that our amplitudes produce no imaginary part, we must have $\xi < 4$, or

$$M_1 > m_\rho/2 \tag{27}$$

The quark mass we evaluate later in the present section indeed satisfies this condition. This also sets an upper limit for L_π:

$$L_\pi \leq 2.5 \begin{bmatrix} 1/3 \\ 1 \\ 1 \end{bmatrix} \tag{28}$$

For case I, we have rather a small value for L_π, which however, does not necessarily mean a small cut-off Λ_π, if $-\bar{A}$ is large. g_ρ and L_ρ are functions of ξ. In the limit of vanishing external meson mass or $\xi \to 0$, we obtain from (21) and (22)

$$g_\rho(0) = \frac{f_\rho}{2} \begin{bmatrix} 1 \\ 1 \\ 1 \end{bmatrix} = 2.8 \begin{bmatrix} 1 \\ 1 \\ 1 \end{bmatrix} \tag{29}$$

and

$$L_\rho(0) = \frac{8\pi^2}{f_\rho^2} \begin{bmatrix} 1 \\ 1 \\ 3 \end{bmatrix} = \begin{bmatrix} 2.5 \\ 2.5 \\ 1.6 \end{bmatrix}, \tag{30}$$

where we have taken $f_\rho = 5.6$. [16]

$g_\rho(\xi)$ and $L_\rho(\xi)$ are plotted in Fig. 1 and Fig. 2, where ξ is limited to $\xi < 4$, corresponding to (27).

Finally we discuss a tricky problem of determining the apparent quark mass M_1.

For this we turn to the $\rho^o \to \pi^+\pi^-$ triangle diagram to define the coupling constant $f_{\rho\pi\pi}$. Here, both cut-off parameters Λ_π and L_π are involved. How to cut-off in this case is unambiguously prescribed in methods 2 illustrated in the appendix, while an ad hoc postulate must be made in method 1. We notice from (26) and (30) that $L_\pi << L_\rho$ in cases I and III, and $L_\pi \sim L_\rho$ in case II. If $L_\pi << L_\rho$, we expect the lower one, L_π, gives an effective cut-off and this is confirmed in the case of method 2. Then in each case, the cut-off will be given roughly by L_π. Thus

$$f_{\rho\pi\pi} = \begin{bmatrix}3\\1\\1\end{bmatrix} \frac{g_\pi^2}{2\pi^2} g_\rho \left[\bar{L} + \frac{1}{2} I_o(\xi) - 2I_1(\xi)\right], \tag{31}$$

where

$$\bar{L} = L_\pi + \varepsilon. \tag{32}$$

ε is a small positive number representing a possible error in using L_π as the effective cut-off. Setting $\xi = 0$ and using (20) and (29), we have

$$f_{\rho\pi\pi} = f_\rho \left(1 + \begin{bmatrix}3\\1\\1\end{bmatrix} \frac{g_\pi^2}{4\pi^2} \varepsilon\right). \tag{33}$$

Since the relation $f_{\rho\pi\pi} = f_\rho$ holds within experimental errors [17], we will take $\varepsilon = 0$ in the following. Conversely speaking, a physically reasonable assumption that $\bar{L} = L_\pi$ leads to the universality relation of the vector meson dominance model

$$f_{\rho\pi\pi} = f_\rho . \tag{34}$$

Now keeping ξ finite, setting $\bar{L} = L_\pi$, and using (20) and (25), Eq.(31) can be written as

$$f_{\rho\pi\pi} = f_\rho \frac{g_\rho(\xi)}{g_\rho(o)} \left\{ 1 + \begin{bmatrix}3\\1\\1\end{bmatrix} \frac{1}{4\pi^2} \frac{M_1^2}{f_\pi^2} \left[\frac{1}{2} I_o(\xi) - 2I_1(\xi)\right] \right\} \tag{35}$$

which determines M_1 as a function of ξ. This is plotted in Fig. 3. The values of ξ and therefore M_1 are determined from the intersects of the curves $M_1^2 = M_1{}^2(\xi)$ and $M_1{}^2 = m_\rho^2/\xi$, and we get

$$\xi = \begin{bmatrix} 3.95 \\ 2.85 \\ 3.83 \end{bmatrix} \qquad M_1 = \begin{bmatrix} 385 \\ 453 \\ 391 \end{bmatrix} \quad \text{MeV} . \tag{36}$$

With these values of ξ and M_1, g_ρ and g_π are determined from Fig. 1 and Eq. (25) as

$$g_\rho = \begin{bmatrix} 0.9 \\ 2.0 \\ 1.7 \end{bmatrix} , \qquad g_\pi = - \begin{bmatrix} 4.1 \\ 4.9 \\ 4.2 \end{bmatrix} \tag{37}$$

The cut-off parameters are determined from Fig. 2 and (26) as

$$L_\pi = \begin{bmatrix} 0.8 \\ 1.7 \\ 2.2 \end{bmatrix} \qquad L_\rho = \begin{bmatrix} 5.8 \\ 2.7 \\ 10.5 \end{bmatrix} \tag{38}$$

IV. Test of the Parameters and Models

We study $\pi^o \to 2\gamma$, $\eta \to 2\gamma$, $\eta' \to 2\gamma$, $\omega \to \pi^o + \gamma$, $\omega \to 3\pi$ and mass splittings of 0^- and 1^- octets as tests of parameters obtained in Sec. III and also as tests of the three models. As for the radiative decays of π^o, η, η', and ω, in the limit of $\xi = 0$, we obtain the same expressions as were used in O. For this part, we will repeat very briefly the conclusions of O for the sake of completeness.

For $\pi^o \to 2\gamma$, the triangle diagram gives [4]

$$T_\pi = - \frac{e^2}{4\pi} \left(\frac{g_\pi}{M_1} \right) m_\pi \begin{bmatrix} 1 \\ -1 \\ 1/3 \end{bmatrix} = \frac{\alpha}{\pi} \frac{m_\pi}{f_\pi} \begin{bmatrix} 1 \\ -1 \\ 1/3 \end{bmatrix} \tag{39}$$

where we have used (25). The cases I and II give a decay rate $\Gamma_{\pi \to 2\gamma} = 7.65$ eV

whereas the experimental value is 7.74 (1±0.12) eV [18]. If we believe in an analysis of sign of $T_\pi f_\pi$ by Okubo [19], the case II is excluded, but the analysis may not be completely conclusive.

The $\eta \to 2\gamma$ and $\eta' \to 2\gamma$ amplitudes can also be calculated likewise. Here we have to take into account of a small singlet-octet mixing. Introducing mixing angle θ by

$$|\eta\rangle = \cos\theta\,|\eta_8\rangle + \sin\theta\,|\eta_o\rangle$$

$$|\eta'\rangle = -\sin\theta\,|\eta_8\rangle + \cos\theta\,|\eta_o\rangle \tag{40}$$

where $|\eta_8\rangle$ and $|\eta_o\rangle$ are pure octet and singlet states we obtain

$$T_\eta = \frac{\alpha}{\pi}\frac{m_\pi}{f_\pi\sqrt{3}}\frac{1}{}\left\{\begin{bmatrix}1\\-1\\1/3\end{bmatrix}\cos\theta + 2\sqrt{2}\begin{bmatrix}2\\1\\1/\sqrt{3}\end{bmatrix}\sin\theta\right\}$$

$$= \frac{T_\pi^{(I)}}{\sqrt{3}}\begin{bmatrix}2.1\\-0.41\\0.50\end{bmatrix}, \tag{41}$$

$$T_{\eta'} = \frac{\alpha}{\pi}\frac{m_\pi}{f_\pi}\frac{1}{\sqrt{3}}\left\{-\begin{bmatrix}1\\-1\\1/3\end{bmatrix}\sin\theta + 2\sqrt{2}\begin{bmatrix}2\\1\\1/3\end{bmatrix}\cos\theta\right\}$$

$$= \frac{T_\pi^{(I)}}{\sqrt{3}}\begin{bmatrix}5.4\\3.0\\0.86\end{bmatrix}, \tag{42}$$

where we have used a mixing angle $\theta \simeq 11^\circ$ as was determined from the mass fit[20]. These give decay widths

$$\Gamma_{\eta\to 2\gamma} = \begin{bmatrix}0.76\\0.033\\0.043\end{bmatrix}\ \text{KeV and}\ \Gamma_{\eta'\to 2\gamma} = \begin{bmatrix}25.6\\8.2\\0.67\end{bmatrix}\ \text{KeV} \tag{43}$$

whereas experimental data give [18]

$$\Gamma^{exp}_{\eta \to 2\gamma} = 1.01 \pm 0.25 \text{ and } \Gamma_{\eta', \to 2\gamma} < 264 \pm 148 \text{ KeV}.$$

The large contribution of the singlet component in case I is due to the fact that all S, U and B components of the singlet contribute additively. In case II, singlet and octet contributions tend to cancal leading to the strong suppression of T_η. Unless an argument for reversing the sign of θ is put forth, case II is in great difficulty. Case III fails again as in $\pi^o \to 2\gamma$ because of the suppression factor 1/3 resulting from the fractional charges of quarks.

$\omega \to \pi^o\gamma$ is given by a triangle diagram similar to that of $\pi^o \to 2\gamma$ but here we have to keep ξ finite. We obtain [21]

$$f_{\omega\pi\gamma} = \begin{bmatrix}3\\1\\1\end{bmatrix} \frac{eg_\rho}{4\pi^2} \frac{g_\pi}{M_1} m_\pi J(\xi)$$

$$= -\begin{bmatrix}3\\1\\1\end{bmatrix} \frac{f_\rho}{2e} \left(\frac{\alpha}{\pi} \frac{m_\pi}{f_\pi}\right) \left[\frac{g_\rho(\xi)}{g_\rho(o)} J(\xi)\right] \tag{44}$$

with

$$J(\xi) = -\frac{1}{\xi} \int_o^{'} \frac{dx}{x(1-x)} \ell n \left[1-\xi x(1-x)\right] \tag{45}$$

At $\xi = 0$, case I gives $f_{\omega\pi\gamma} = \frac{3f_\rho}{2e} T_\pi^{(I)}$, the same result as in vector meson dominance model which gives $\Gamma_{\omega \to \pi^o\gamma} = 0.56(1 \pm 0.13)$ MeV about two standard deviation below the experimental data. Again in this limit, cases II and III are worse off. The finite mass effect does not change the results at $\xi = 0$ drastically, because the reduced value of g_ρ is offset by an enhancement due to $J(\xi)$.

$$\frac{g_\rho(\xi)}{g_\rho(o)} J(\xi) = \begin{bmatrix}0.77\\1.0\\1.1\end{bmatrix} \tag{46}$$

The factor $J(\xi)$ is as large as 2.5 for $\xi = 4$. The enhancement is due to the fact that $m_\omega \simeq m_\rho$ is close to the pseudo-threshold $\rho(\omega) \to q + \bar{q}$. One could doubt the physical reality of such an effect, in which case we should limit ourselves entirely to $\xi = 0$. The reduction of the value of g_ρ for finite ξ is originally due to the same effect. However, we would like to take the view point that the finiteness of ξ reflects a physical reality in the following sense. The actual quark mass may be very large but inside a hadron they move with the small effective mass we found within a certain broad potential barrier. We consider that the ground state 0^- octet and 1^- nonet are stable bound systems of $q\bar{q}$ inside the barrier, neglecting decay channels. The quark-loop diagrams may then be considered as representing local propagations of quarks inside the barrier.

It is of some interest to examine the $\omega \to 3\pi$ amplitude by a quark-loop diagram although higher order corrections to such a four-point loop are expected fairly large. We obtain [22]

$$T_{\omega 3\pi} = \begin{bmatrix}3\\1\\1\end{bmatrix} \frac{g_\rho}{2\pi^2} \left(\frac{g_\pi}{M_1}\right)^3 m_\pi^3 K(\xi)$$

$$= \begin{bmatrix}3\\1\\1\end{bmatrix} \frac{f_\rho}{4\pi^2} \left(\frac{m_\pi}{f_\pi}\right)^3 \left[\frac{g_\rho(\xi)}{g_\rho(o)} K(\xi)\right] \qquad (47)$$

Here $K(\xi)$ is an enhancement factor similar to $J(\xi)$ in (45), but is hard to calculate for general values of π momenta. We may expect that its effect is again cancelled partly by reduction of g_ρ. Neglecting the last bracket in (47), we get

$$T_{\omega 3\pi} \simeq \begin{bmatrix}1.3\\0.44\\0.44\end{bmatrix} \qquad (48)$$

A numerical evaluation of $K(\xi)$, which is, in fact, a function of ξ and appropriate products of the pion momenta, is greater than 4 and can be as large as 10 in the phase space of $\omega \to 3\pi$. An average value $K(\xi) \simeq 5$ is reasonable. If we

take this value, then

$$T_{\omega 3\pi} = \begin{bmatrix} 2.1 \\ 0.71 \\ 0.71 \end{bmatrix} \tag{49}$$

To obtain the observed width of ω, we must have $T_{\omega 3\pi} \simeq 3.6 \pm 0.9$. Again case I is relatively favored. It seems that there is a consistent tendency for quark-loop diagrams to underestimate amplitudes involving ω meson.

Finally, we shall examing a perturbation calculation of SU_3 mass splitting of 0^- and 1^- octets by means of quark-loop diagrams. As an unperturbed system we will take the 0^- octet and the 1^- nonet degenerate with the physical π and ρ, respectively. The p- (n-) quark mass M_1 is given by (36). The perturbation energy is then the mass difference of λ and p quarks, $\delta M_1 = M_3 - M_1$. The interaction Hamiltonian which gives rise to (strong interaction) mass splittings of the mesons is

$$H' = \delta M_1 \{ \bar{S} \begin{bmatrix} 0 & & \\ & 0 & \\ & & 1 \end{bmatrix} S + \bar{U} \begin{bmatrix} 0 & & \\ & 0 & \\ & & 1 \end{bmatrix} U + \bar{B} \begin{bmatrix} 0 & & \\ & 0 & \\ & & 1 \end{bmatrix} B \} \tag{50}$$

for cases I and II; and

$$H' = \delta M_1 \bar{q} \begin{bmatrix} 0 & & \\ & 0 & \\ & & 1 \end{bmatrix} q \tag{51}$$

for case III. A triangle diagram involving (50) or (51) and two K meson vertices (The unperturbed K mass degenerate with that of π.) gives

$$\delta m_\pi^2 = \begin{bmatrix} 3 \\ 1 \\ 1 \end{bmatrix} \frac{g_\pi^2}{2\pi^2} M_1 \delta M_1 L_\pi = \begin{bmatrix} 1 \\ 1 \\ 1 \end{bmatrix} 2 M_1 \delta M_1 \tag{52}$$

Finite terms have been dropped safely, as $\xi = m_\pi^2/M_1^2 << 1$. There is some ambiguity as to what value we should use for δm_π^2. The right hand side of (52) which may be written as δM_1^2 suggests that we take

$$\delta m_\pi^2 = 2 m_\pi \delta m_\pi = 2(m_k - m_\pi) m_\pi \simeq 0.1 \text{ GeV}^2, \tag{53}$$

while taking $\delta m_\pi^2 = m_k^2 - m_\pi^2$, we get $\delta m_\pi^2 \simeq 0.22\ \text{GeV}^2$. We will use the value (53), which gives from (52)

$$M_1 \delta M_1 = 0.05\ \text{GeV}^2. \tag{54}$$

Using M_1 given in (36), we find

$$\delta M_1 \simeq \begin{bmatrix} 133 \\ 110 \\ 128 \end{bmatrix} \text{MeV} \tag{55}$$

These values are close to $m_\phi - m_{k^*} \simeq m_{k^*} - m_\rho \sim 127$ MeV.

A triangle diagram involving K^* is finite, and gives

$$\delta m_\rho^2 = \begin{bmatrix} 3 \\ 3 \\ 1 \end{bmatrix} \frac{g_\rho^2}{2\pi^2} \delta M_1 M_1 \left[-3/2 + 2/\xi\ I_o(\xi) \right]$$

$$= \begin{bmatrix} 3 \\ 3 \\ 1 \end{bmatrix} \frac{f_\rho^2}{16\pi^2} M_1 \delta M_1 \left\{ \left[\frac{g_\rho(\xi)}{g_\rho(0)} \right]^2 \left[-3 + \frac{4}{\xi} I_o(\xi) \right] \right\} . \tag{56}$$

At $\xi = 0$, the last bracket is unity, and we have

$$\delta m_\rho^2 = \begin{bmatrix} 3 \\ 3 \\ 1 \end{bmatrix} \frac{f_\rho^2}{16\pi^2} M_1 \delta M_1 = \begin{bmatrix} 0.03 \\ 0.03 \\ 0.01 \end{bmatrix} \text{GeV}^2. \tag{57}$$

This should be compared with the experimental value

$$\delta m_\rho^2 = 2\ (m_{K^*} - m_\rho)\ m_\rho \simeq 0.19\ \text{GeV}^2. \tag{58}$$

The finite-mass correction factor is huge and is

$$\left[\frac{g_\rho(\xi)}{g_\rho(0)}\right]^2 \left[\frac{4}{3} I_o(\xi) - 3\right] = \begin{bmatrix} 5.2 \\ 3.3 \\ 9.0 \end{bmatrix} \tag{59}$$

which gives

$$\delta m_\rho^2 \simeq \begin{bmatrix} 0.16 \\ 0.1 \\ 0.9 \end{bmatrix} \text{GeV}^2. \tag{60}$$

close enough to the required value (58) in case I. It should be remarked that the factor (59) has a finite limit as $\xi \to 0$, although $g_\rho(\xi) \to 0$ and $\frac{4}{3} I_o(\xi) - 3 \to \infty$ at this piont. The limiting value in case I and II is

$$\delta m_\rho^2 \quad (\xi=4) = 4\ \delta M_1 M_1 = 2.0\ \text{GeV}^2.$$

V. Concluding Remarks

Under the assumption that static mesonic amplitudes are dominated by the lowest order quark loop diagrams, we reaffirmed the Okubo's conclusion that Gell-Mann-Zweig model consistently underestimates mesonic radiative decay amplitudes and that the Namba-Han model with a charm singlet assignment for the pseudoscalar and the vector mesons yields a right order of magnitude for these amplitudes. In view of the importance of the result, a critical examination of our fundamental assumption will be necessary. Let us take $\pi^o \to 2\gamma$ amplitude as an example, for which the G-Z model gives a value 1/3 of that of the N-H model. Besides our quark loop amplitude (1), which we may call T_π^{quark}, we can also consider diagrams involving hadronic intermediate states, like baryon loop diagrams, which we denote by T_π^{hadron}. Our Assumption of the quark loop dominance amounts to either

$$T_\pi = T_\pi^{\text{quark}} = T_\pi^{\text{hadron}} \tag{61}$$

or

$$T_\pi = T_\pi^{\text{quark}},\ T_\pi^{\text{hadron}} = 0. \tag{62}$$

The former relation may be called complementary, in that we have two ways of evaluating the same thing. We can find an analogous situation if we remark that in duality terminology T_π^{quark} corresponds to the Veneziano amplitude and T_π^{hadron} to the higher order unitarity diagrams. The relation between the residue of poles in the Veneziano amplitudes and the absorptive part of all the unitarity diagrams could quite conceivably be of the complementary type like (61). In any case all calculations termed as quark models, including quark parton models, do neglect hadronic intermediate states, and ours is within this general context of the quark models.

The above considerations show that in order to save the G-Z model we must abandon either the assumption of minimal electromagnetic interaction for quarks [23] (we will not discuss this possibility here), or our fundamental assumption of quark loop dominance and assume instead that

$$T_\pi = T_\pi^{quark} + T_\pi^{hadron} \tag{63}$$

In the G-Z model, then, T_π^{hadron} should be the main part, and this is quite possible in view of the fact that the nucleon loop diagram alone accounts for the required T_π. It is extremely instructive to compare Eq.(63) with another evaluation of T_π obtained by one of the authors (BLY) [24] from the point of the dispersion relation in the two photon mass variables. There we have two terms, vector meson pole terms (simultaneous poles in both photon channels) T_π^{pole}, corresponding to T_π^{hadron} and a subtraction term (single pole terms) T_π^{ETC}, which is determined by the equal time commutators of spatial components of electromagnetic current (BJL limit).

$$T_\pi = T_\pi^{ETC} + T_\pi^{pole} \tag{64}$$

From the point of the pure vector meson dominance model, we have $T_\pi^{ETC} = 0$ and T_π^{pole} is given by ω-ρ poles (Gell-Mann, Sharp and Wagner model [25]), which gives a reasonable fit of T_π. If we use quark algebra on the other hand, we have

$$T_\pi^{ETC} = 8\pi\alpha \frac{f_\pi m_\pi^2}{m_\rho} \quad S \tag{65}$$

which is very close to (1) in value. In fact equating both, we obtain a good relation

$$m_\rho^2 = 8\pi^2 f_\pi^2 \tag{66}$$

In the G-Z model T_π^{ETC} is again small and ω-ρ pole term in T_π^{pole} dominates T_π. If we take the N-H model in (64), then T_π^{pole} must be small as T_π^{ETC} alone accounts for T_π. Such possibility was explored before [12]. However, it would be more logical, from the point of quark models, to doubt the validity of 'hybrid' relations like (63) and (64), as discussed below.

Finally we would like to speculate on a physical situation in which our scheme might be justified. Since quarks have not been detected at extremely high energies, as in the CERN ISR, the quarks must have an extremely high mass, or even an infinite mass. Thus, we may call the quark field as a non-asymptotic, or quasi-nonasymptotic field, in the sense that quarks do not propagate asymptotically. If we want to describe an amplitude and its intermediate states in terms of asymptotic fields, we should not include quarks into such states. Eq.(63) and (64) lose their validity and we have instead $T_\pi = T^{hadron}$ or $T_\pi = T^{pole}$. How do we obtain a quark description then? We imagine that quarks are trapped permanently in hadrons. In a hadron, quarks must move with a small effective mass inside a certain broad trapping barrier. Our quark loop diagrams must be regarded as describing approximately local propagation of quarks inside the barrier. In a rigorous treatment, we would have to talk in terms of excitation into discrete levels in the barrier rather than free particle-like propagations. The nature of the complementarity between hadronic and quark descriptions can be understood by considering the absorptive part of a hadronic amplitude. In our quark model, a hadronic transition occurs via an excitation of trapped quarks into higher states and their eventual decays into hadronic channels. The transition rate can be obtained by just the excitation cross section of quarks, the decay prohability being 100 %. It remains to be seen how good our approximation of the free quark propagation with a small effective mass will be. For that, we will have to know the nature and mechanism of the trapping barrier.

Acknowledgement

One of the authors (HS) would like to thank Professors H. Joos, E. Lohrmann and W. Paul for their hospitalities extended to him at DESY. Thanks are also due to Professor H. Joos and Dr. F. Gutbrod for valuable discussions on the quark models. The other author (BLY) would like to thank Professor D.A. Geffen and M. Hamermesh for their hospitality at the Department of Physics of the University of Minnesota, where part of this work was performed in the summer of 1971.

Appendix

Two cut-off methods will be discussed in this appendix.

Method 1. Finite range integration

This is by far the simplest of all the cut-off methods. In this method, Feynman integrals are simply performed in a finite sphere of radius Λ in the Euclidean space after the Wick rotation is performed. The well known ambiguity in shifting the origin of the integration variable, when a given Feynman integral is (superficially) lineraly divergent or more singular [26], can only produce finite constants in all the cases we considered; it does not affect the $\ln \Lambda^2$ terms. A consistent set of A_i, the momentum independent finite constant terms, can be calculated by choosing a certain prescription for evaluating the divergent Euclidean integrals. We use the prescription described in Akhiezer and Berestetsky; [27] it gives

$$L = \ln \frac{\Lambda 2}{M_1^2} - 1, \qquad \overline{A} = -1 \tag{A.1}$$

Another class of cut-offs can be constructed by taking into account the possible non-point like structure of the meson-quark-quark vertex when the quark 4-momenta are large. Such a construction has to satisfy the analyticity and spectral function constraints of a vertex function. It can be given the meaning for a representation of hadronic wave functions. For example, instead of a point coupling, the meson-quark-quark vertex can be put into the following form:

$$\Gamma(k_1^2, k_2^2) = \int_0^1 dz \int_0^\infty d\sigma \frac{f(z,\sigma)}{\sigma - zk_1^2 - (1-z)k_2^2} \tag{A.2}$$

where k_1 and k_2 are the momenta of the quarks; the normalization of the function $f(z,\sigma)$ is

$$\int_0^1 dz \int_0^\infty d\sigma \frac{f(z,\sigma)}{\sigma} = 1 \tag{A.3}$$

We also add the symmetry condition

$$f\ (z,\sigma) = f\ (1-z,\sigma) \tag{A.4}$$

Method 2. We take (A.2) - (A.4) and choose

$$f\ (z,\sigma) = \Lambda^4 \delta'(\sigma-\Lambda^2) \tag{A.5}$$

which leads to the following form for the meson-quark-quark vertex:

$$\Gamma(k_1^2,\ k_2^2) = \frac{\Lambda^2}{k_1^2-\Lambda^2} \cdot \frac{\Lambda^2}{k_2^2-\Lambda^2} \tag{A.6}$$

In the present method we insert (A.6) at all the meson-quark-quark vertices (not at the current current-quark-quark vertices). For example in the $\pi^+ \to \mu^+ \nu$ two-point loop, (A.6) is inserted at the pion vertex and obviously the cut-offs are applied independently to the two quark propagators. In this case $\overline{A} = 2$ and

$$L = \ln\left(\frac{\Lambda^2}{M_1^2}\right) - 2 \tag{A.7}$$

There are other cut-off methods, for example, the Feynman cut-off [28], or more generally the Pauli-Villars regularization method [29]. They lead to the results $\overline{A} = \Delta A_i = 0$ when in the former a gauge condition is implemented for the ρ-γ two-point loop. We shall not elaborate them further.

In table 1, we list the values of $\overline{A}$ and ΔA_i for several diagrams See, Eqs.(2)-(6)

Table 1. Values of $\bar{A}$ and ΔA_i

method	1	2
$\bar{A}$	-1	-2
$\pi^+ \to \mu^+ \nu$	0	0
$\pi \to \pi\ \gamma$	1/2	-7/12
$\rho \to \gamma$	1/6	1/3
$\rho \to \rho\gamma$	-5/6	1/12

References and Footnotes

1. D.D. Sutherland, Nucl.Phys. B2, 433 (1967).

2. S. Adler, Phys.Rev. 177, 2622 (1969); S. Adler and W. Bardeen, Phys.Rev. 182, 1517 (1969).

3. S.Adler, reference 2; J. Schwinger, Phys.Rev. 82, 664 (1951).

4. The normalization of T_π is such that the invariant decay matrix element for $\pi^o \to \gamma(k_1,\varepsilon_1) + \gamma(k_2,\varepsilon_2)$ is.

$$M = \frac{T_\pi}{m_\pi} \varepsilon_{\mu\nu\lambda\rho} \varepsilon_1^\mu \varepsilon_2^\nu k_1^\lambda k_2^\rho$$

which gives the decay width formula $\Gamma_{\pi^o \to 2\gamma} = (T_\pi)^2 m_\pi / 64\pi$.

5. S. Okubo, in Proceedings of the Internal Conference on Symmetries and Quark Models (Wayne State University 1969), Gordon and Breach 1970.

6. J. Steinberger, Phys.Rev. 76, 1180 (1949); H. Fukuda and Y.Miyamoto, Prog. Theor. Phys. 4,347 (1949).

7. M.L. Goldberger and S.B. Treiman, Phys. Rev. 110,1178 (1958); 111, 354 (1958).

8. C.H. Llewellyn Smith, Ann.Phys. 53, 521 (1969); T. Gudehus, Phys.Rev. 184, 1788 (1969); T. Kitazoe and T. Teshima, Nuovo Cimento 57A, 497 (1968); M. Bohm, H. Joos and M. Krammer, Nuovo Cimento 7A, 21 (1972); Z. Maki and I. Umemura, Prog.Theor. Physics 45, 530 (1971). Other references can be found in a review talk by G. Morpurgo, Lecture notes at 1971 Erice Summer School.

9. Y. Fujii, Prog.Theor.Phys. 21, 232 (1958).

10. M. Y. Han and Y. Nambu, Phys.Rev. 139, 1006 (1965); see also, Cabibbo, L. Maimi and G. Preparate, Phys. Letters 25 B, 132 (1967).

11. We would like to stress this point in view of the recent paper by Lipkin [H.J. Lipkin, Phys.Rev. Letters, 28, 63 (1972)] , who argued a suppression of C-current in deep inelastic scattering from the assumption that all low lying hadrons are charm singlet. We can, however, expect a large charm-symmetry breaking from a vector-gluon quark interaction which involves the eighth component of a charm spin.

12. K. Johnson, F. E.Low, and H. Suura, Phys.Rev. Letts. 18, 1224 (1967); J.D. Bjorken, Phys. Rev. 160, 1582 (1967); N. Cabibbo, L. Maimi and G. Preparata, Phys.Letters 25 B, 31 (1967); E.S. Abers, D.A. Dicus, R.E. Newton and H.R. Quinn, Phys. Rev. 167, 1461 (1967).

13. One might worry how a ρ meson composed of S.U.B pairs can decay into π mesons which are $B\bar{B}$ pairs. Obviously we need a fairly strong charm symmetric interaction working in 1^- mesons, which couples $S\bar{S}$, $U\bar{U}$ and $B\bar{B}$ pairs. The situation here is analogous to a classical set of coupled pendulums, only one of which is subjected to damping.

14. Jun Otakazawa and H. Suura, Phys.Rev. Letters 21, 1295 (1968).

15. The ρ^o-γ coupling is defined by em_ρ^2/f_ρ. See, for instance J.J. Sakuai, Currents and Mesons PP65-71 (The University of Chicago Press, 1969).

16. The value of f_ρ can be summarized as follows: (a) The colliding beam data gives $f_\rho = 5.13(\pm 0.07)$, (See, S.C.C. Ting, in Proceeding of the 14th International Conference on High Energy Physics, Vienna, Austria, Sept. 1969, edited by J. Prentki and J. Steinberger). (b) From ρ^o-Photoproduction it gives $f_\rho = 5.3(1\pm0.08)$ (H. Alvensleben, et al, Phys.Rev. Letters 24, 786 (1970)) and $f_\rho = 5.55(1\pm0.11)$ (H.J. Behrend, et.al., Phys.Rev. Letters 24, 336 (1970). (c) From the vector meson universality, the $\rho^o \to 2\pi$ width gives $f_\rho = \gamma_{\rho\pi\pi} = 5.51(1\pm0.09)$ (d) A recent ρ-ω interference experiment with the colliding beam, by the Orsay group gives a value for f_ρ close to that determined in (c) (An extensive symmary for the experimented determination of f_ρ up to 1969 can be found in E. Lohrmann, Lund International Conference on Elementary Particles, 1969.

17. See Ref. 16 and especially part (d)

18. N. Barash-Schmidt et al., Rev. Mod.Phys. 43, No.2, Part II, April, 1971. We used the experimental value $f_\pi \simeq 93$ MeV.

19. S. Okubo, Phys. Rev. 179, 1629 (1969); See also F.J. Gilman, ibid 184, 1964 (1969).

20. R.H. Dalitz, in Les Houches Summer School Lecture Notes 1969, Gordon and Breach 1970.

21. $f_{\omega\pi\gamma}$ is defined by

$$\langle \gamma_1 k_1 \varepsilon | \; j_\pi(0) | \omega, p\varepsilon' \rangle = \frac{f_{\omega\pi\gamma}}{m_\pi} \; \varepsilon_{\mu\nu\lambda\rho} \; \varepsilon^\mu \; \varepsilon'^\nu \; k^\lambda p^\rho .$$

22. $T_{\omega 3\pi}$ is related to the decay amplitude by

$$M(\omega \to 3\pi) = \frac{T_{\omega 3\pi}}{m_\pi^3} \; \varepsilon_{\mu\nu\lambda\sigma} \; \varepsilon^\mu(\omega) \; k_1^\nu \; k_2^\lambda \; k_3^\rho \quad ,$$

where k_1, k_3 and k_3 are pion momenta.

23. For example, a large quark anomalous moment was introduced in discussing $\omega \to \pi\gamma$, see Becci and Morgurgo, Phs. Rev. 140 B, 687 (1965).

24. Bing-Lin Young, Phys. Rev. 161, 1615 (1967).

25. M. Gell-Mann, D. Sharp and W.G. Wagner, Phys. Rev. Letters 8, 216 (1962).

26. J. M. Tauch and F. Rohrlich, Theory of Photons and Electrons (Addison-Wesley, Reading, Mass.,1955), PP 454-460.

27. A.I. Akheiezer and V.B. Berestetskii, Quantum Electrodynamics, Interscience puhlishers, 1965, PP 631-639.

28. See, for example, R.P. Feynman, Theory of Fundamental Processes, W.A. Benjamin, inc., 1961.

29. W. Pauli and F. Villars, Rev. Mod. Phys. 21, 434 (1949).

Figure captions:

Figure 1. Vector meson-quark-quark coupling as a function of ξ, $0 \leq \xi \leq 4$, for the 3 models.

Figure 2. Vector meson cut-off as a function of ξ.

Figure 3. P-(n-) quark mass as a function of ξ. The values of M_1 are determined from the intersects of the $M(\xi)$ [See Eq.(35)] and $\sqrt{m_\rho^2/\xi}$.

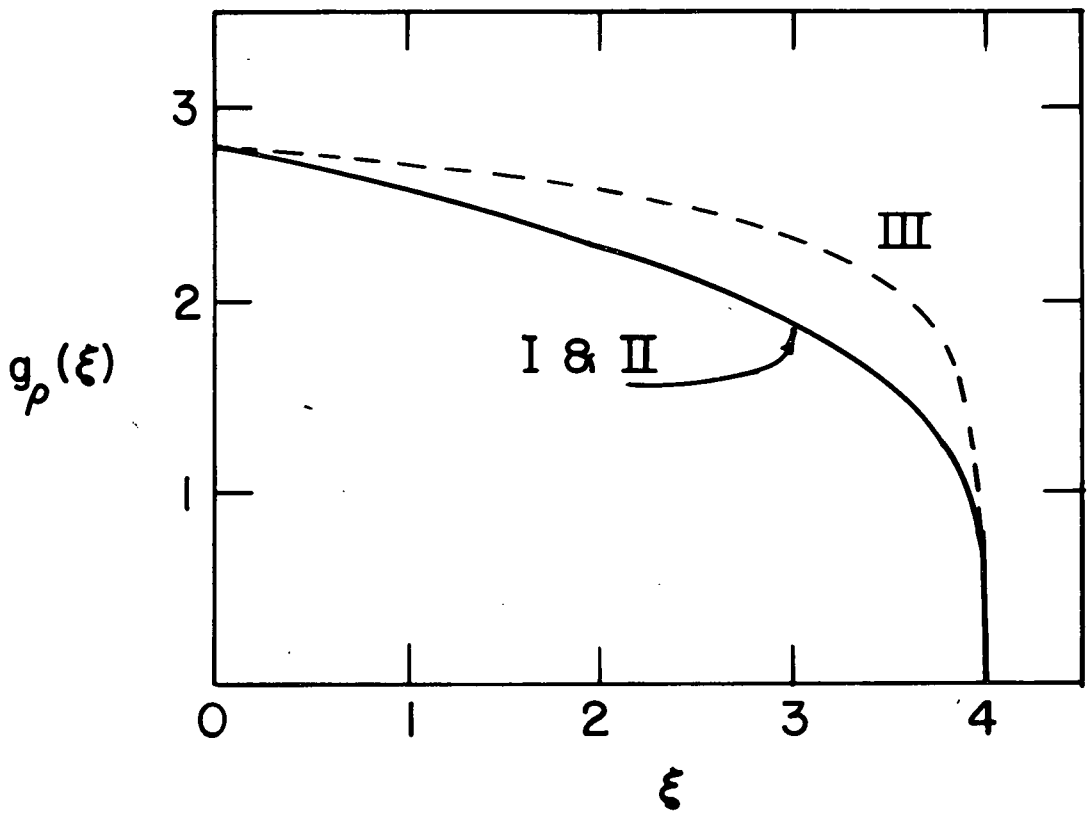

Fig. 1

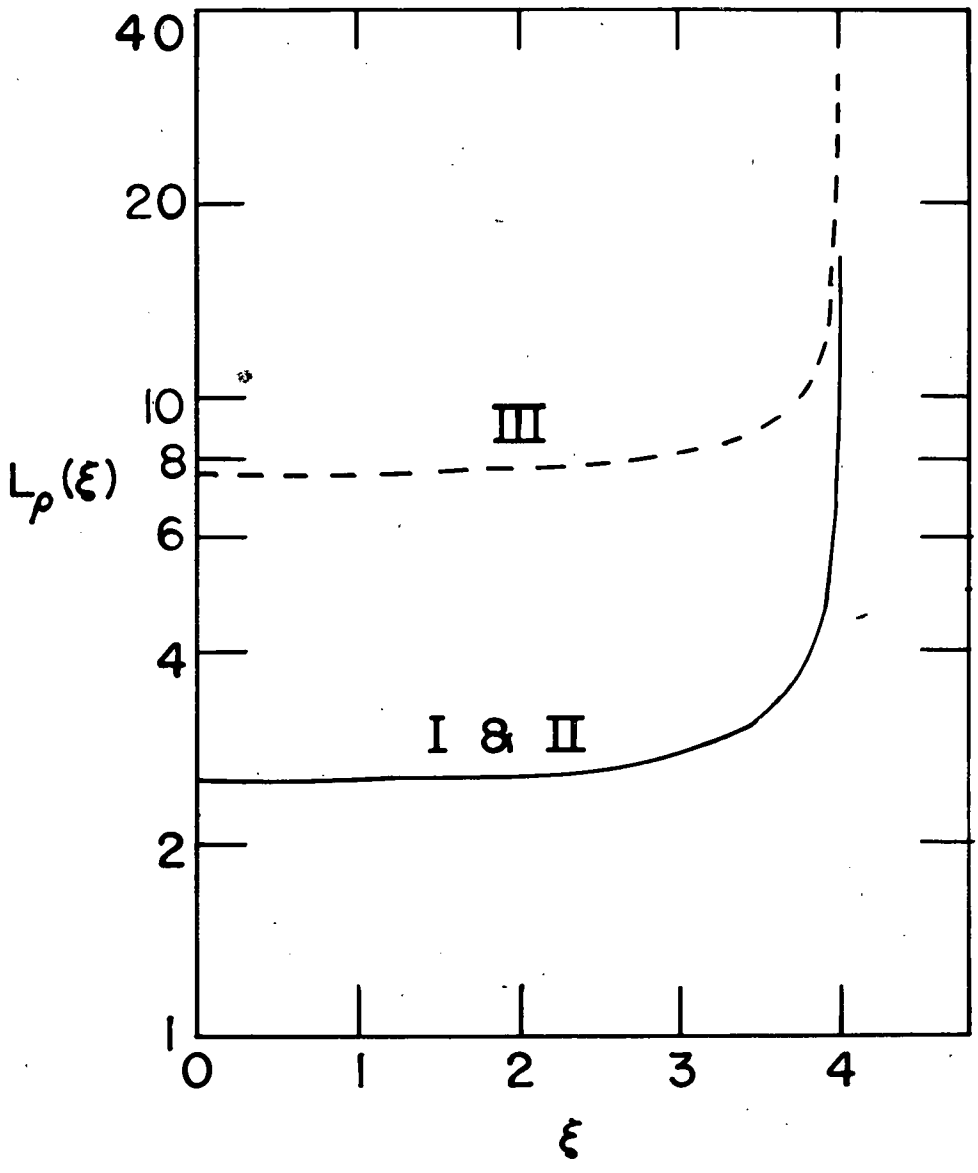

Fig. 2

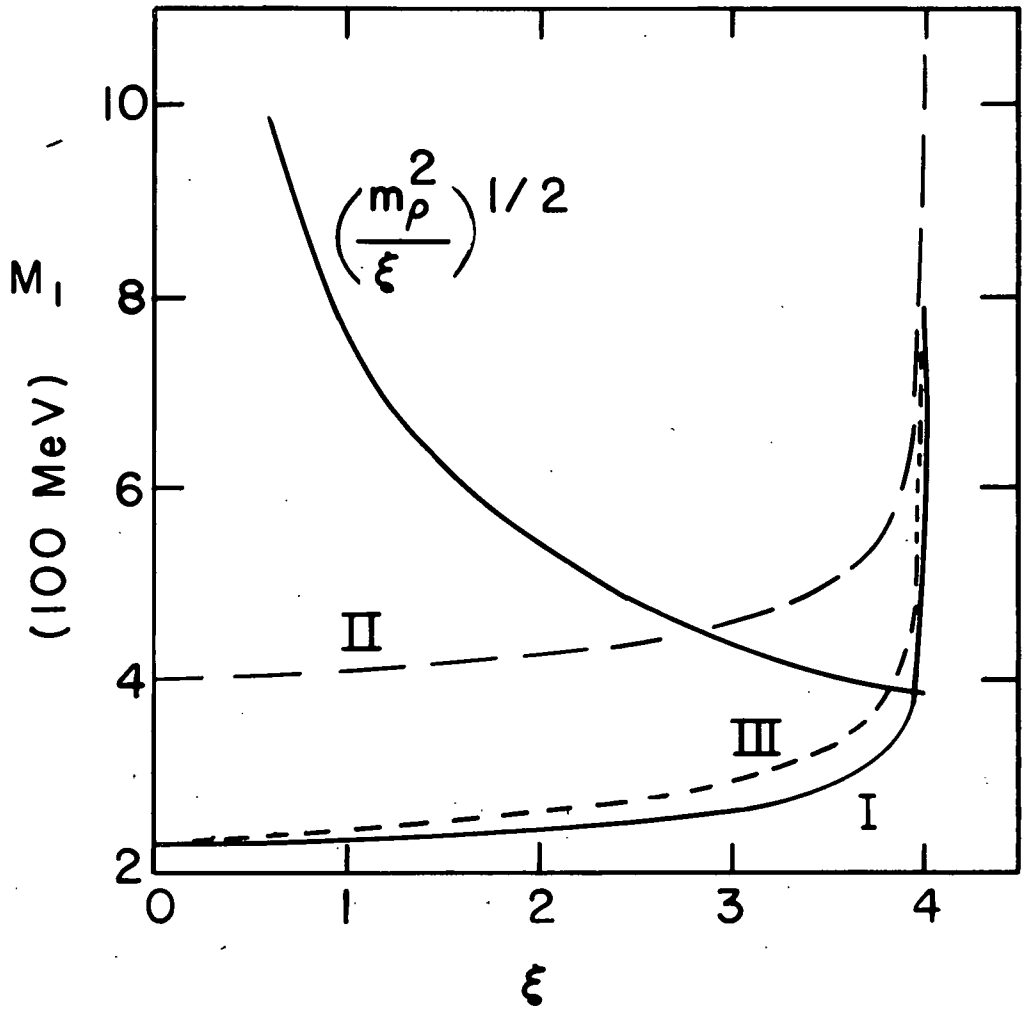

Fig. 3